NASA Technical Memorandum 107231

Progressive Fracture of Fiber Composite Builtup Structures

Pascal K. Gotsis and C.C. Chamis
Lewis Research Center
Cleveland, Ohio

Levon Minnetyan
Clarkson University
Potsdam, New York

Prepared for the
32nd Annual Technical Meeting
sponsored by the Society of Engineering Science
New Orleans, Louisiana, October 29–November 2, 1995

National Aeronautics and
Space Administration

PROGRESSIVE FRACTURE OF FIBER COMPOSITE BUILTUP STRUCTURES

Pascal K. Gotsis and Christos C. Chamis
National Aeronautics and Space Administration
Lewis Research Center, Cleveland, Ohio 44135

and

Levon Minnetyan
Clarkson University
Potsdam, New York 13699-5710

SUMMARY

The damage progression and fracture of builtup composite structures was evaluated by using computational simulation to examine the behavior and response of a stiffened composite $[0/\pm45/90]_{s6}$ laminate panel subjected to a bending load. The damage initiation, growth, accumulation, progression, and propagation to structural collapse were simulated. An integrated computer code (CODSTRAN) was augmented for the simulation of the progressive damage and fracture of builtup composite structures under mechanical loading. Results showed that damage initiation and progression have a significant effect on the structural response. Also investigated was the influence of different types of bending load on the damage initiation, propagation, and final fracture of the builtup composite panel.

INTRODUCTION

The aircraft, marine, and automotive industries use stiffened composite panels because of their low weight, high stiffness, and stability. Design considerations with regard to the durability of stiffened panels require an a priori evaluation of the damage initiation and propagation mechanisms under expected service loads. Concerns for the safety and survivability of critical components require quantification of the composite structural damage tolerance during overloads. Characteristic flexibilities in the tailoring of composite structures make them more versatile for fulfilling structural design requirements. However, these same design flexibilities render the assessment of composite structural response and durability more complex, prolonging the design and certification process and adding to the cost of the final product. It is difficult to evaluate composite structures because of the complexities in predicting their overall congruity and performance, especially when structural degradation and damage propagation occur. The predictions of damage initiation, damage growth, and propagation to fracture are important in evaluating the load-carrying capacity, damage tolerance, safety, and reliability of composite structures. The most effective way to obtain this quantification is through integrated computer codes that couple composite mechanics with structural analysis and damage progression models. The COmposite Durability STRuctural ANalysis (CODSTRAN) computer code was developed for this purpose by integrating and coupling the following disciplines: (1) the mechanics of composites, (2) the structural finite element (FEM) analysis, and damage progression and tracking. CODSTRAN has previously been used to simulate the damage progression in a variety of composite structures: stiffened adhesively bonded composite structures (ref. 1), adhesively bonded concentric composite cylinders (ref. 2), progressive damage and fracture of adhesively bonded pipe joints (ref. 3), damage progression in bolted composite structures (ref. 4), damage tolerance of composite pressurized thin shell structures (refs. 5 to 7), and simulation of Iosipescu shear testing (ref. 8).

To design stiffened panel structures that will be subjected to bending loads, it is important to know how the structures behave and what their catastrophic limits are. By simulating the damage initiation, damage progression, and final fracture of the structure, this report investigates the response of the stiffened composite panel subjected to bending loads.

CODSTRAN METHODOLOGY

CODSTRAN is an integrated computer code in which three modules are coupled: composite mechanics (ICAN), finite element analysis (MHOST), and damage progression modeling. ICAN (Integrated Composite Analyzer) is a composite mechanics computer code (ref. 9) that provides the constituent (fiber and matrix) material properties from an available data bank and computes the ply properties and the composite properties (effective properties) of the laminate in a hygrothermal environment. The code is based on the theory of the micromechanics of composites and the classical laminate theory. ICAN can compute ply stresses by using known stress resultants (force per laminate thickness, where force can be a bending, a twisting, or a concentrated load). In ICAN, two failure criteria were established for the detection of ply failures: (1) the maximum stress criterion in which individual ply failure modes are assessed by ICAN using failure criteria associated with the negative and positive limits of the six ply stress components in the material directions 1 to 3 (fig. 1):

$$S_{\ell 11C} < \sigma_{\ell 11} < S_{\ell 11T} \tag{1}$$

$$S_{\ell 22C} < \sigma_{\ell 22} < S_{\ell 22T} \tag{2}$$

$$S_{\ell 33C} < \sigma_{\ell 33} < S_{\ell 33T} \tag{3}$$

$$S_{\ell 12(-)} < \sigma_{\ell 12} < S_{\ell 12(+)} \tag{4}$$

$$S_{\ell 23(-)} < \sigma_{\ell 23} < S_{\ell 23(+)} \tag{5}$$

$$S_{\ell 13(-)} < \sigma_{\ell 13} < S_{\ell 13(+)} \tag{6}$$

where $S_{\ell ij\alpha}$ represents the ply stress limit (ply strength) in which the ij subscript indicates the stress component and the α subscript indicates the sense as tension and/or compression for normal stresses and as $\pm$ for shear stress limits on the ply; σ is the ply stress. The ICAN composite mechanics module computes $S_{\ell ij\alpha}$ stress limits. (2) The modified distortion energy (MDE) criterion takes into account combined stresses and is expressed as

$$F = 1 - \left[\left(\frac{\sigma_{\ell 11\alpha}}{S_{\ell 11\alpha}} \right)^2 + \left(\frac{\sigma_{\ell 22\beta}}{S_{\ell 22\beta}} \right)^2 - K_{\ell 12} \frac{\sigma_{\ell 11\alpha}}{S_{\ell 11\alpha}} \frac{\sigma_{\ell 22\beta}}{S_{\ell 22\beta}} + \left(\frac{\sigma_{\ell 12S}}{S_{\ell 12S}} \right)^2 \right] \tag{7}$$

where α and β indicate tensile or compressive stress, $S_{\ell 11\alpha}$ is the ply longitudinal strength in tension or compression, $S_{\ell 22\alpha}$ is the transverse strength in tension or compression, and

$$K_{\ell 12} = \frac{(1 + 4\nu_{\ell 12} - \nu_{\ell 13})E_{\ell 22} + (1 - \nu_{\ell 23})E_{\ell 11}}{\left[E_{\ell 11}E_{\ell 22}(2 + \nu_{\ell 12} + \nu_{\ell 13})(2 + \nu_{\ell 21} + \nu_{\ell 23})\right]^{1/2}} \tag{8}$$

The type of failure is assessed by comparing the magnitudes of the squared terms in equation (7). Depending on the dominant term in the MDE failure criterion, fiber failure or matrix failure is assigned. If the first squared term in equation (7) that corresponds to ply longitudinal tensile or compressive failure is dominant, fiber failure is assigned. On the other hand, if one of the other squared terms corresponding to ply transverse tensile or compressive failure or to ply shear failure is dominant, matrix failure is assigned. In ICAN, the described failure modes of the plies are failure due to fiber fracture in tension or in compression; damage due to matrix fracture in tension or in compression; and damage due to intralaminar shear fracture.

MHOST is a finite element computer code (ref. 10) used to solve structural analysis problems. The code can perform linear or nonlinear static and dynamic analyses. MHOST has a library containing a variety of elements, among which is the four-node shell element used for the present work. By supplying the boundary conditions, the type of analysis desired, the applied loads, and the laminate properties (using ICAN), MHOST performs the structural analysis. In addition, MHOST provides the computed stress resultants to the ICAN code, which then computes the developed ply stresses for each ply and checks for ply failure.

The damage progression module monitors composite degradation for the entire structure and relies on ICAN for composite micromechanics, macromechanics, and laminate analysis. In this module, the overall evaluation of the composite structural durability is conducted.

The CODSTRAN simulation cycle is shown in figure 2. Proceeding clockwise along the left side, one sees the constituent material properties (fiber and matrix) provided by ICAN's data base, the ply properties computed from the micromechanics theory, and the laminate properties computed from the laminate theory. These properties in conjunction with the finite element mesh, the loads, and the boundary conditions are incorporated in MHOST, which performs the structural analysis and provides the computed stress resultants to ICAN (right side of the figure). ICAN uses the laminate theory to compute the ply stresses and to check for ply failure.

The nonlinear structural analysis in the MHOST code is performed in conjunction with an incremental load algorithm. The load is increased in small increments (equilibrium positions). In each position, a number of iterations (incremental damages) are performed (fig. 3) and the structure is checked for ply failure. If damage is detected, the model is automatically updated with a new finite element mesh and new laminate properties; then another finite element analysis is performed and the iterations continue until no further damage occurs (equilibrium position). At this point, the load is increased and the above procedure repeated until the final failure of the structure. The damage progression, fracture, and collapse of the structure are monitored during this procedure.

The CODSTRAN code is written in FORTRAN 77 computer language for UNIX operating systems at the NASA Lewis Research Center.

FIBER COMPOSITE BUILTUP STRUCTURE

The composite structure used for this investigation is a panel stiffened by a hat-type stringer that is well bonded to the skin. The finite element model (fig. 4) uses a four-node shell element, the boundary conditions for which are a fixed end on one side (in the x-direction) and a free end at the other side. The cross-sectional geometry and physical dimensions of the stiffened panel are shown in figure 5. The panel and hat of the structure are made of the same high-strength AS-4 graphite fibers (table I) in a high-modulus, high-strength (HMHS) epoxy matrix (table II). The skin laminate of the structure consists of forty-eight 0.132-mm (0.00521-in.) plies, resulting in a composite thickness of 6.35 mm (0.25 in.). The width of the stiffened panel is 330.2 mm (13 in.) and the length is 279.4 mm (11 in.). The fiber volume ratio is 0.60. The laminate configuration is $[0/\pm45/90]_{s6}$. The 0° plies are in the axial direction of the stiffener, along the x-axis (fig. 4). A negative bending load (with respect to y-axis) was applied at the free edge of the structure and was increased gradually (fig. 4). Damage initiation and progression were monitored as the panel was gradually loaded. For comparison, another case with a positive bending load (with respect to the y-axis) was examined.

RESULTS AND DISCUSSION

The normalized damage progression of the stiffened panel as a function of the normalized applied load (max. catastrophic load due to the positive bending load is 2.208 k-m (19.54 ksi)) is shown in figure 6. In CODSTRAN, damage is defined as the volume of the damaged plies divided by the total volume of the structure. In figure 6, the depicted points of the damage versus the bending load are the equilibrium points that were referred to in the section CODSTRAN Methodology. For both loading conditions, the structural damage is identical, except at the collapse load where the structure with the negative bending load fractured first. The discussion of the composite panel damage initiation and progression for both loading conditions follows.

The damage initiation began at 0.43 of the catastrophic positive bending load (2.208 k-m or 19.54 ksi) for both loading conditions at the front part of the panel where the panel and the stiffener are in contact (figs. 7 and 8).

At the first load increment, for the negative bending load case (fig. 7), damage occurred as a result of matrix failure in tension (MFT) in the 4th and 5th (90°) plies whereas fiber fracture in compression (FFC) occurred in the 48th (0°) ply. At the second load increment, damage occurred because of MFT in the 2d and 3d (±45°) plies and at the 12th and 13th (90°) plies, and failure due to FFC occurred in the 4th and 5th (90°) plies. At the third load increment, failure due to FFC occurred in the 12th and 13th (90°) plies.

In the positive bending load case (fig. 8), at the first load increment, failure due to FFC occurred in the 1st (0°) ply and damage due to MFT occurred in the 44th and 45th (90°) plies. At the second load increment, damage due to MFT occurred in the 36th and 37th (90°) plies, 43d and 47th (–45°) plies, and the 46th (45°) ply; failure due to FFC occurred in the 44th and 45th (90°) plies.

The damage progressed slowly in the front area of the panel until the applied load became equal to 0.74 of the catastrophic load. Increasing the load further caused the damage and the fracture to propagate rapidly until the load became equal to 0.78 of the catastrophic load.

The catastrophic load for the stiffened panel subjected to the negative bending load was 0.88 of the catastrophic load due to the positive bending load. When that load was reached, the front part of the panel broke because of the extended fracture of the fibers. The display of the fractured panel subjected to the negative bending load is shown in figure 9.

For the negative bending load case, the computed ply stresses were plotted using PATRAN postprocessing capabilities for the damage initiation stage. The plot was restricted to the stresses of the top (0°) and the 3rd (–45°) ply, respectively. Including all the plies would have been too time consuming.

At the top ply (0°), the ply stresses were plotted in the longitudinal (fig. 10) and transverse (fig. 11) directions of the fibers. In both figures, high stresses were generated in front of the panel at the contact region with the stiffener.

At the third ply (–45°, the direction formed by the fibers with respect to the x-axis), the ply stresses were plotted in the longitudinal (fig. 12) and transverse (fig. 13) directions of the fibers. The intralaminar shear stresses are shown in figure 14. The results show that high stresses occurred in front of the panel at the contact region with the stiffener.

SUMMARY

The CODSTRAN (COmposite Durability STRuctural ANalysis) computer code was used to evaluate the structural and damage progression responses of a stiffened $[0/\pm45/90]_{s6}$ laminate composite panel. The following results were obtained:

1. Damage initiation began for both bending loads at an applied load equal to 0.43 of the catastrophic positive bending load (at the front edge of the panel stiffener). In the case of the negative bending load, the damage started in the 4th and 5th (90°) plies as a result of matrix fracture in tension and in the 48th (0°) ply as a result of fiber fracture in compression. In the case of the positive bending load, the damage began at the 1st (0°) ply because of fiber fracture in compression and at the 44th and 45th (90°) plies because of matrix fracture in tension.
2. The damage progressed slowly until the applied load was 0.74 of the catastrophic load; thereafter, the damage growth propagated very rapidly until the load was 0.78 of the catastrophic load.
3. The catastrophic load due to the negative bending load was 0.88 of the collapse load due to the positive bending load. When the collapse load was reached for the negative bending case, the front part of the panel broke as a result of extended fiber fracture.

REFERENCES

1. Gotsis, P.K.; Chamis, C.C.; and Minnetyan, L.: Effect of Combined Loads in the Durability of a Stiffened Adhesively Bonded Composite Structure. Proceedings of the 36th AIAA/ASME/ASCE /AHS/ASC Structures, Structural Dynamics, and Materials Conference, AIAA–95–1283–CP, part 2, 1995, pp. 1083–1092.
2. Minnetyan, L.; and Gotsis, P.K.: Progressive Fracture in Adhesively Bonded Concentric Cylinders. Proceedings of the 40th International SAMPE Symposium and Exhibition, Anaheim, California, vol. 40, book 1, 1995, pp. 849–860.

3. Chamis, C.C.; Gotsis, P.K.; and Minnetyan, L.: Progressive Damage and Fracture of Adhesively Bonded Fiber Composite Pipe Joints. Energy Week Conference and Exhibition, Symposium on Composite Materials Design and Analysis. Sponsored by ASME, book V, legend V, 1996, pp. 401–408.
4. Chamis, C.C.; Gotsis, P.K.; and Minnetyan, L.: Damage Progression in Bolted Composite Structures. Proceedings of the USAF Structural Integrity Program Conference, 1995. Proceedings in publication.
5. Chamis, C.C.; Gotsis, P.K.; and Minnetyan, L.: Damage Tolerance of Composite Pressurized Shells. Proceedings of the 37th AIAA/ASME/ASCE/AHS/ASC Structures, Structural Dynamics, and Materials Conference, AIAA–96–1556–CP, part 4, 1996, pp. 2112–2121.
6. Gotsis, P.K.; Chamis, C.C.; and Minnetyan, L.: Defect Tolerance of Pressurized Fiber Composite Shell Structures. Proceedings of the 41st International SAMPE Symposium and Exhibition, vol. 41, 1996, pp. 450–461.
7. Gotsis, P.K.; Chamis, C.C.; and Minnetyan, L.: Progressive Fracture of Fiber Composite Thin Shell Structures Under Internal Pressure and Axial Loads. NASA TM–107234, 1996.
8. Minnetyan, L., et al.: Progressive Fracture of Composite Subjected to Iosipescu Shear Testing. Accepted for publication at the Proceedings of the 13th Symposium on Composite Material: Testing and Design, 1996.
9. Murthy, P.L.N.; Ginty C.A.; and Sanfeliz, J.G.: Second Generation Integrated Composite Analyzer (ICAN) Computer Code. NASA TP–3290, 1993.
10. Nakazawa, S.: MHOST User's Manual, version 4.2, vol. 1, NASA CR–182235, 1989.

TABLE I.—AS–4 GRAPHITE FIBER PROPERTIES

Number per end	10 000
Diameter, mm (in.)	0.00762 (0.300×10^{-3})
Density, kg/m^3 ($lb/in.^3$)	4.04×10^{-7} (0.063)
Normal modulus, GPa (psi)	
Longitudinal	227 (32.90×10^6)
Transverse	13.7 (1.99×10^6)
Poisson's ratio	
ν_{12}	0.20
ν_{23}	0.25
Shear modulus, GPa (psi)	
G_{12}	13.8 (2.00×10^6)
G_{23}	6.90 (1.00×10^6)
Thermal expansion coefficient, /°C (/°F)	
Longitudinal	1.0×10^{-6} (-0.55×10^{-6})
Transverse	1.0×10^{-6} (-0.56×10^{-6})
Heat conductivity, J-m/hr/m^2/°C (BTU-in./hr/$in.^2$/°F)	
Longitudinal	43.4 (580)
Transverse	4.34 (58)
Heat capacity, J/Kg/°C (BTU/lb/°F)	712 (0.17)
Strength, MPa (ksi)	
Tensile	3723 (540)
Compressive	3351 (486)

TABLE II.—HMHS EPOXY MATRIX PROPERTIES

Density, kg/m^3 (lb/in.^{3})	3.40×10^{-7} (0.0457)
Normal modulus, GPa (ksi)	4.27 (629)
Poisson's ratio, ν	0.34
Coefficient of thermal expansion, /°C (/°F)	0.72 (0.4×10^{-4})
Heat conductivity, J-m/hr/m^2/°C (Btu-in./hr/in.^{2}/°F)	930 (1.25)
Heat capacity, J/kg/°C (Btu/lb/°F)	738 (0.25)
Strength, MPa (ksi)	
Tensile	84.8 (12.3)
Compressive	423 (61.3)
Shear	148 (21.4)
Allowable strain	
Tensile	0.02
Compressive	0.05
Shear strain	0.04
Torsional	0.04
Void conductivity, J-m/hr/m^2/°C (Btu-in./hr/in.^{2}/°F)	16.8 (0.225)
Glass transition temperature, °C (°F)	216 (420)

TABLE III.—PLY STRENGTH OF AS-4/HMHS
[Fiber direction, parallel to ply 1 material axis; tension, T; compression, C; material axes of ply, 1 to 3.]

Ply stress component	Strength	
	MPa	ksi
$S_{\ell 11T}$	1930.30	280
$S_{\ell 11C}$	1475.85	210
$S_{\ell 22T}$	91.38	13
$S_{\ell 22C}$	228.27	33
$S_{\ell 12}$	65.57	9.5
$S_{\ell 23}$	59.98	8.7

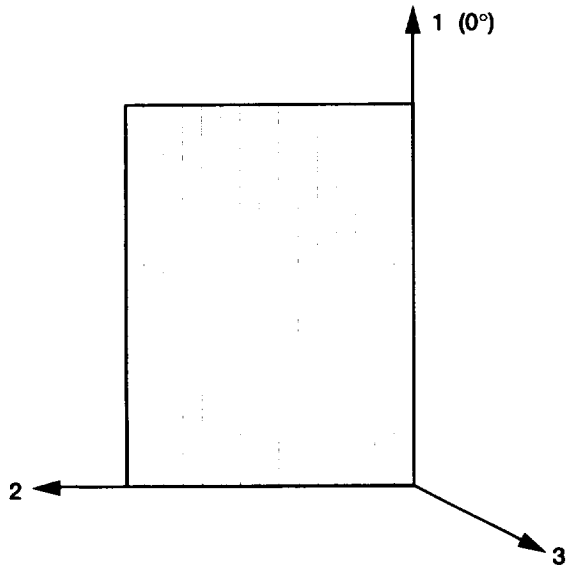

Figure 1.—Ply with fibers and material axes.

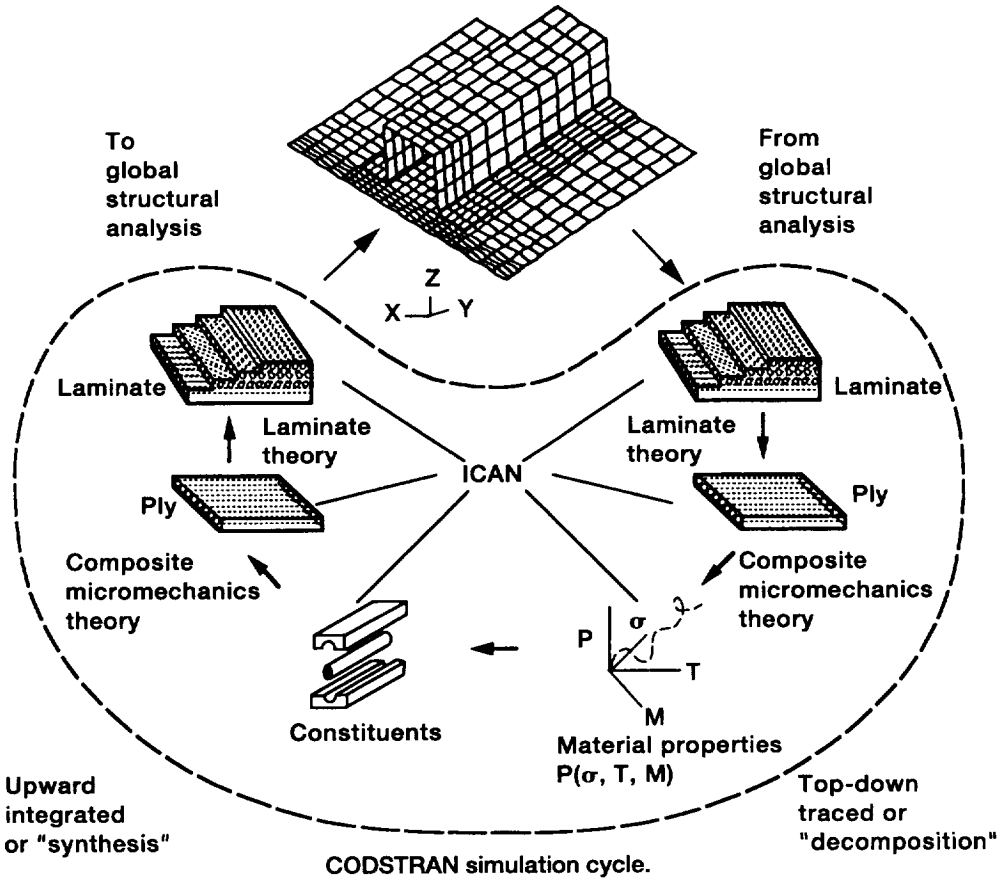

Figure 2.—Integrated composite analysis.

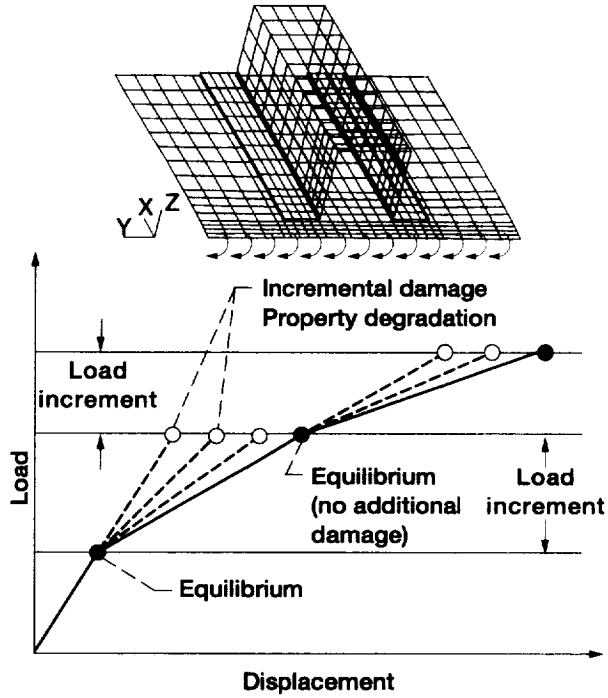

Figure 3.—CODSTRAN load incrementation.

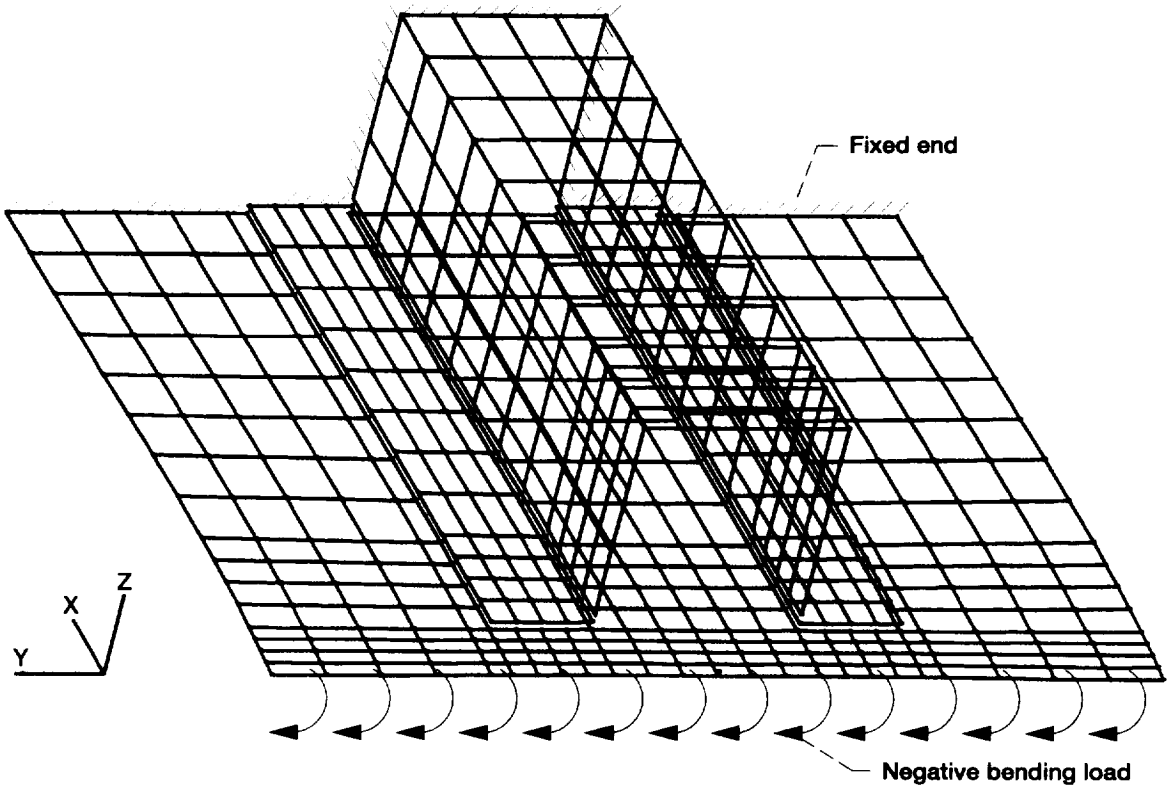

Figure 4.—Finite element model.

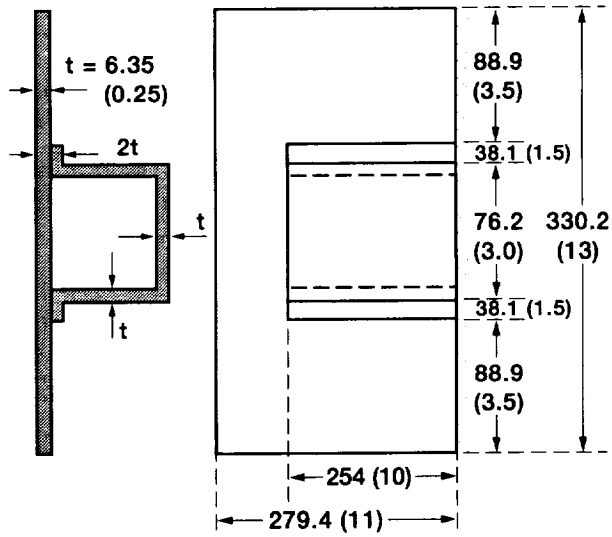

Figure 5.—Geometry of builtup structures. Plate and stiffener, AS-4/HMHS; configuration, $[0/\pm45/90]_{s6}$; 48 plies; fiber volume ratio, 0.60. All dimensions are in mm (in.).

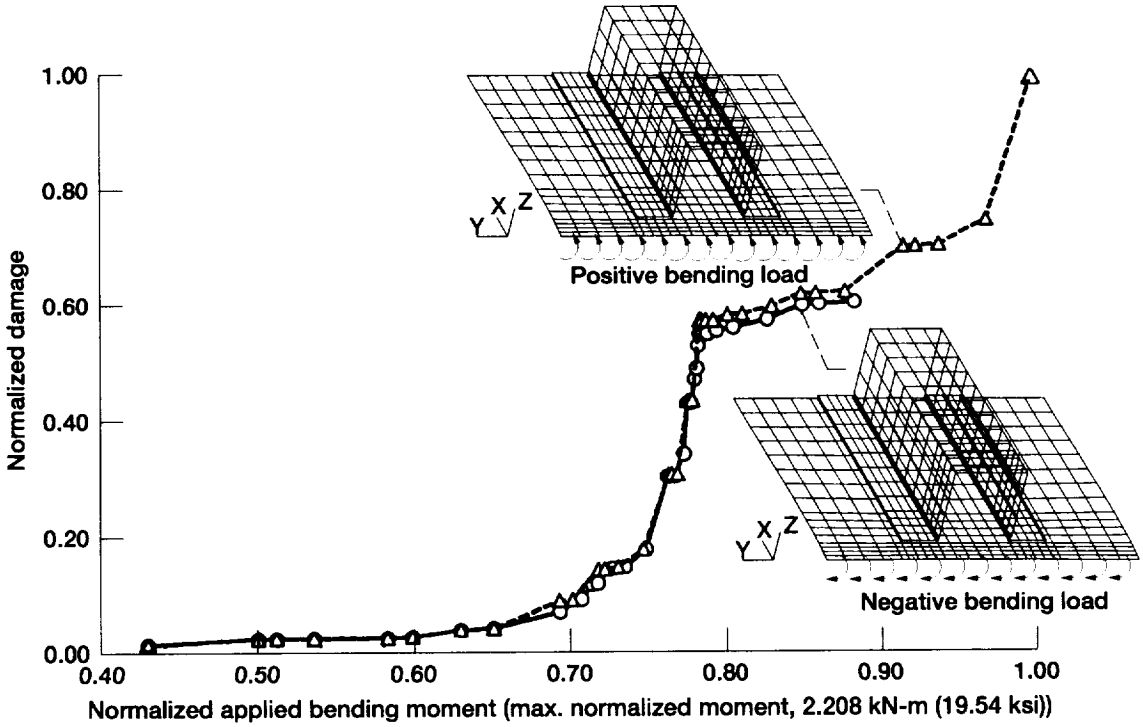

Figure 6.—Damage versus applied load for graphite/epoxy stiffened panel $[0/\pm45/90]_{s6}$.

DAMAGE INITIATION

Ply	Angle, deg	Incremental damage[a]		
		First	Second	Third
1	0	-----	-----	-----
2	45	-----	MFT	-----
3	-45	-----	MFT	-----
4	90	MFT	FFC	-----
5	90	MFT	FFC	-----
---	----	-----	-----	-----
---	----	-----	-----	-----
---	----	-----	-----	-----
12	90	-----	MFT	FFC
13	90	-----	MFT	FFC
---	----	-----	-----	-----
---	----	-----	-----	-----
—	----	-----	-----	-----
48	0	FFC	-----	-----

[a]MFT, matrix fracture in tension; FFC, fiber fracture in compression.

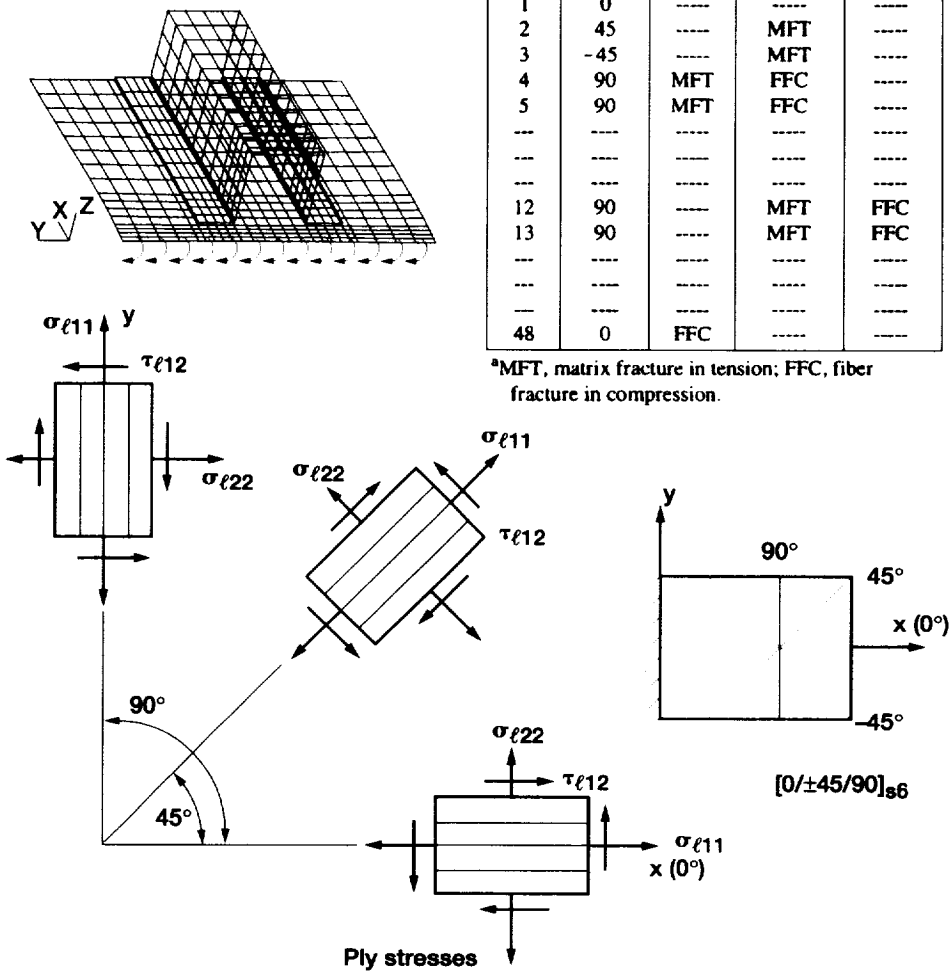

Figure 7.—Failure modes due to negative bending during damage initiation.

DAMAGE INITIATION

Ply	Angle, deg	Incremental damage[a]	
		First	Second
1	0	-----	-----
---	-----	-----	-----
---	-----	-----	-----
---	-----	-----	-----
36	90	-----	MFT
37	90	-----	MFT
---	----	-----	-----
---	----	-----	-----
---	-----	-----	-----
43	-45	-----	MFT
44	90	MFT	FFC
45	90	MFT	FFC
46	45	-----	MFT
47	-45	-----	MFT
48	0	-----	-----

[a]MFT, matrix fracture in tension; FFC, fiber fracture in compression.

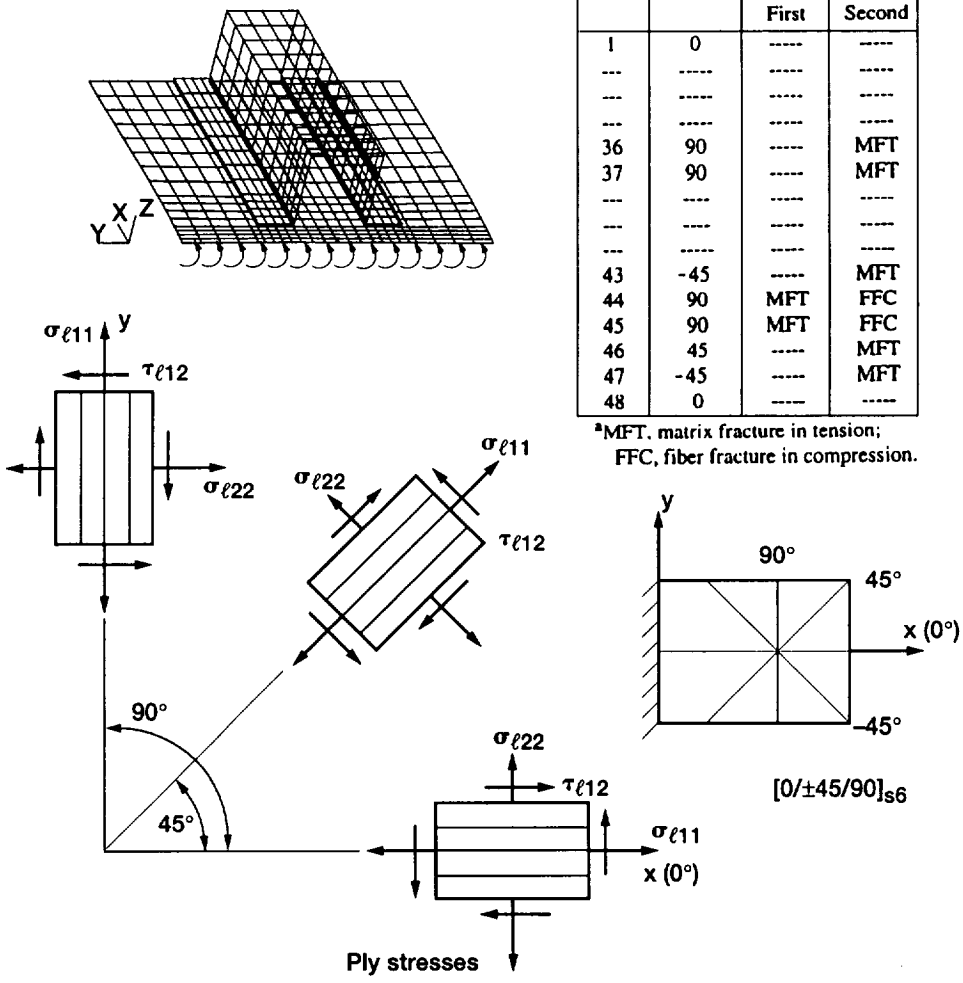

Figure 8.—Failure modes due to positive bending during damage initiation.

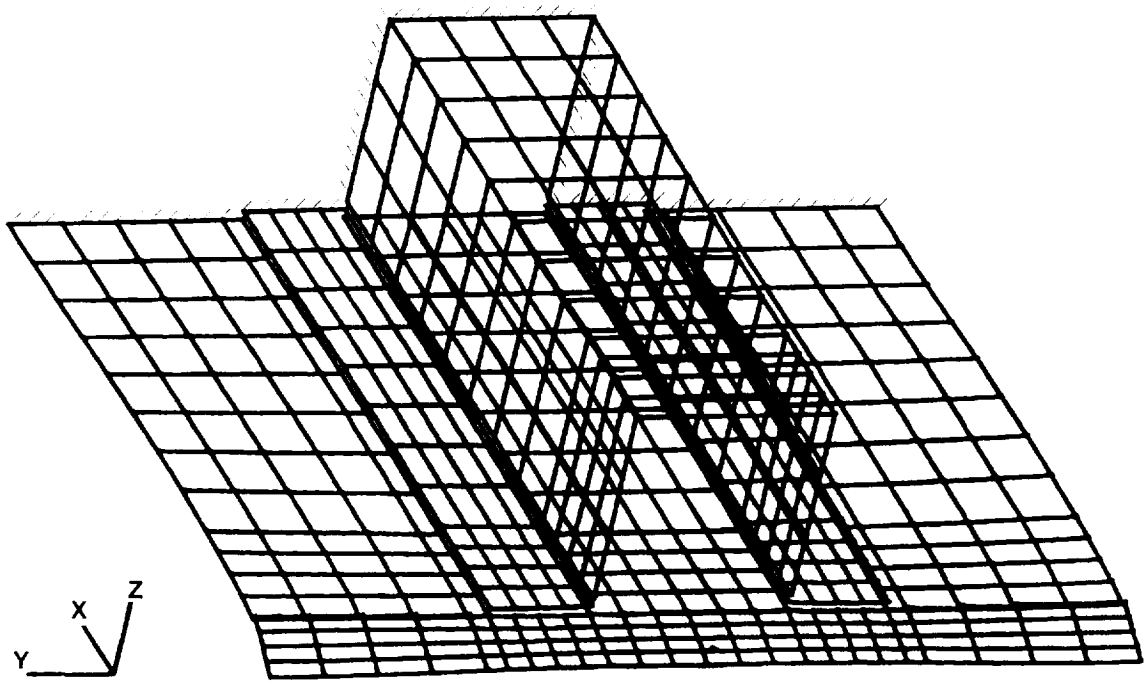

Figure 9.—Fractured builtup panel subjected to negative bending load. Fracture load, 1.97 kN-m (17.29 lb-in.).

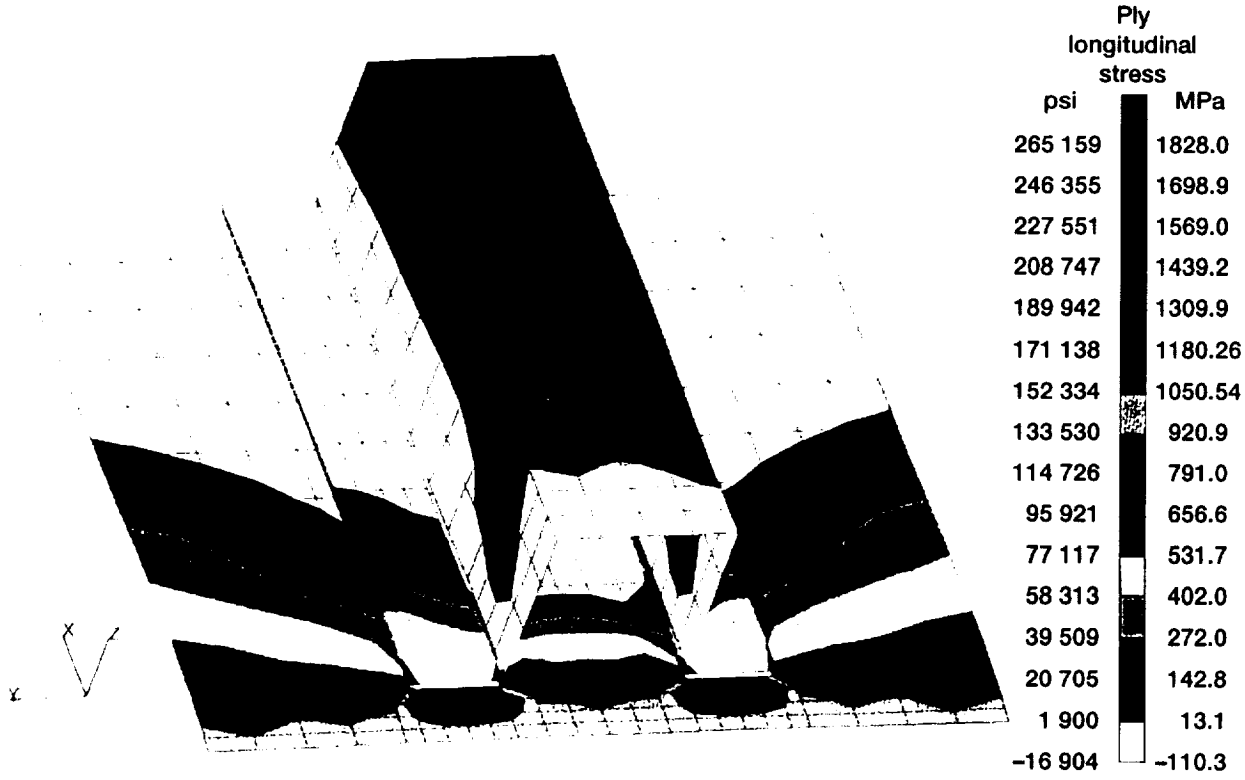

Figure 10.—Ply longitudinal stresses at top ply (0°) during damage initiation for graphite/epoxy panel $[0/\pm45/90]_{s6}$. Applied load, 974.5 N-m (8385 lb-in.).

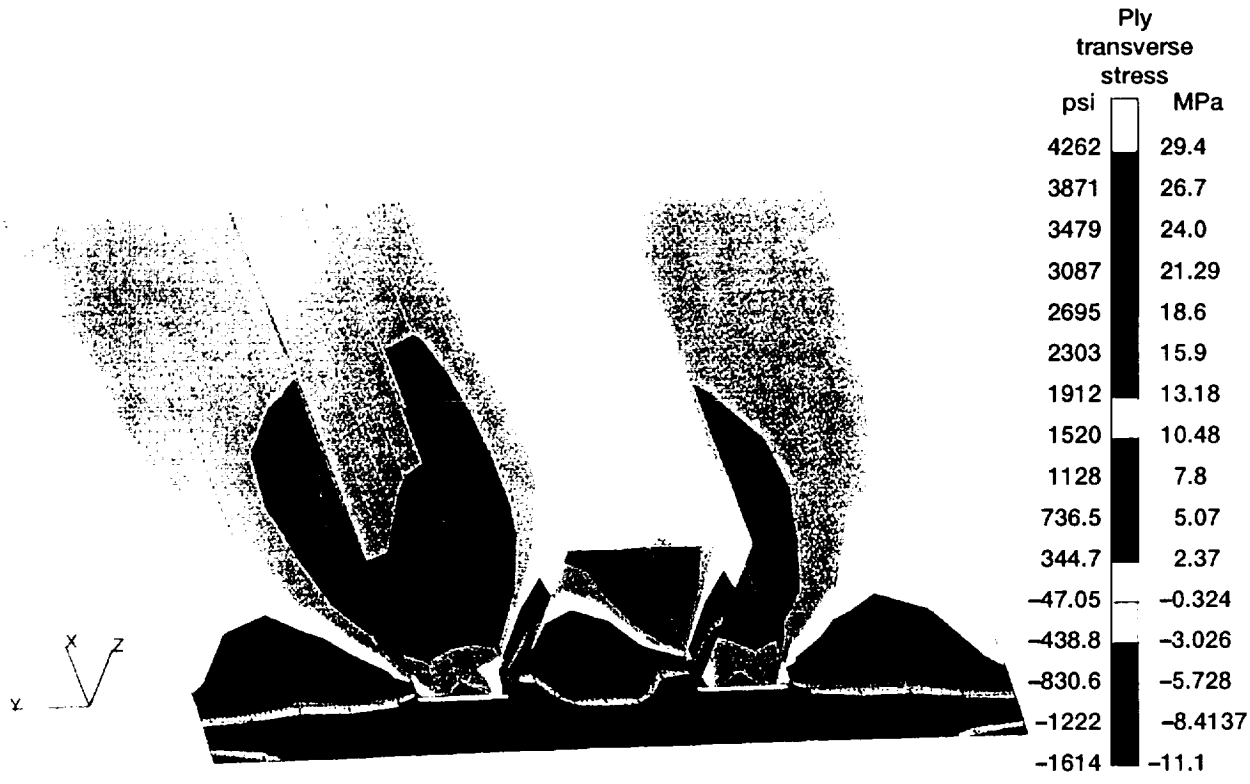

Figure 11.—Ply transverse stresses at top ply (0°) during damage initiation for graphite/epoxy panel $[0/\pm45/90]_{s6}$. Applied load, 974.5 N-m (8385 lb-in.).

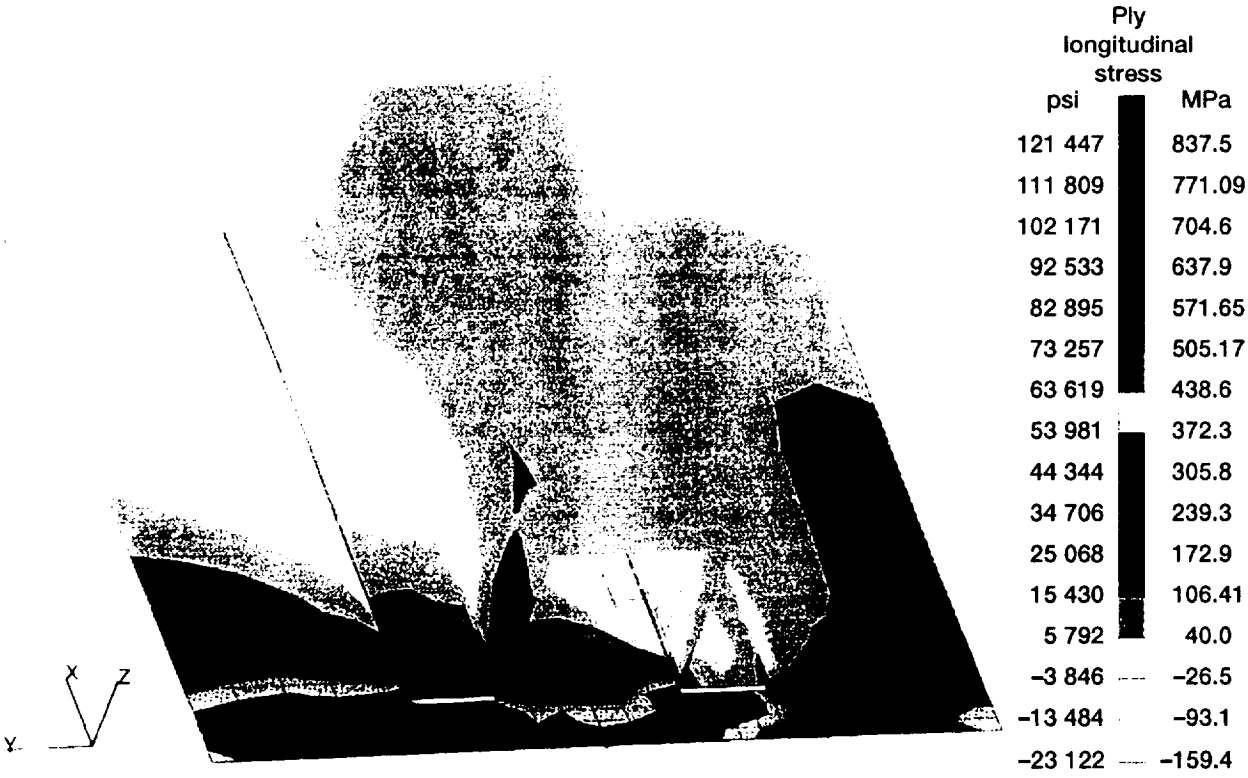

Figure 12.—Ply longitudinal stresses at third ply (–45°) during damage initiation for graphite/epoxy panel $[0/\pm45/90]_{s6}$. Applied load, 974.5 N-m (8385 lb-in.).

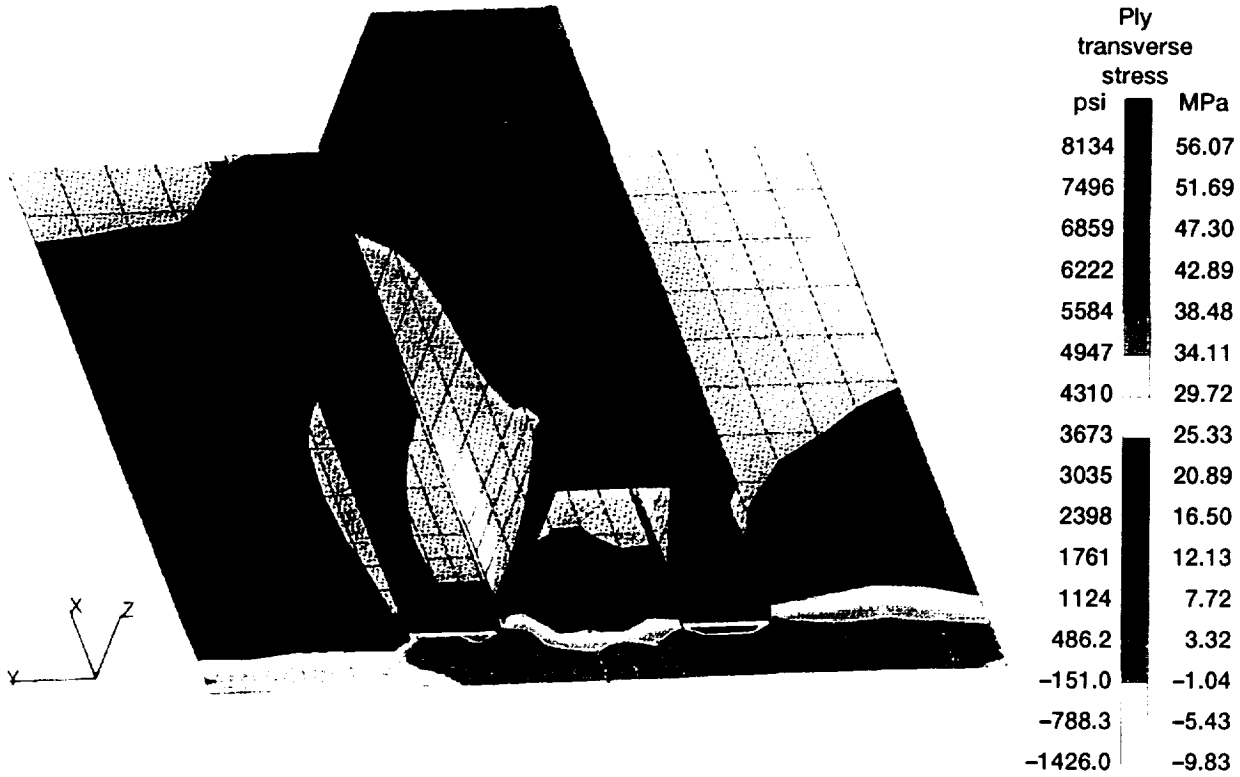

Figure 13.—Ply transverse stresses at third ply (–45°) during damage initiation for graphite/epoxy panel $[0/\pm45/90]_{s6}$. Applied load, 974.5 N-m (8385 lb-in.).

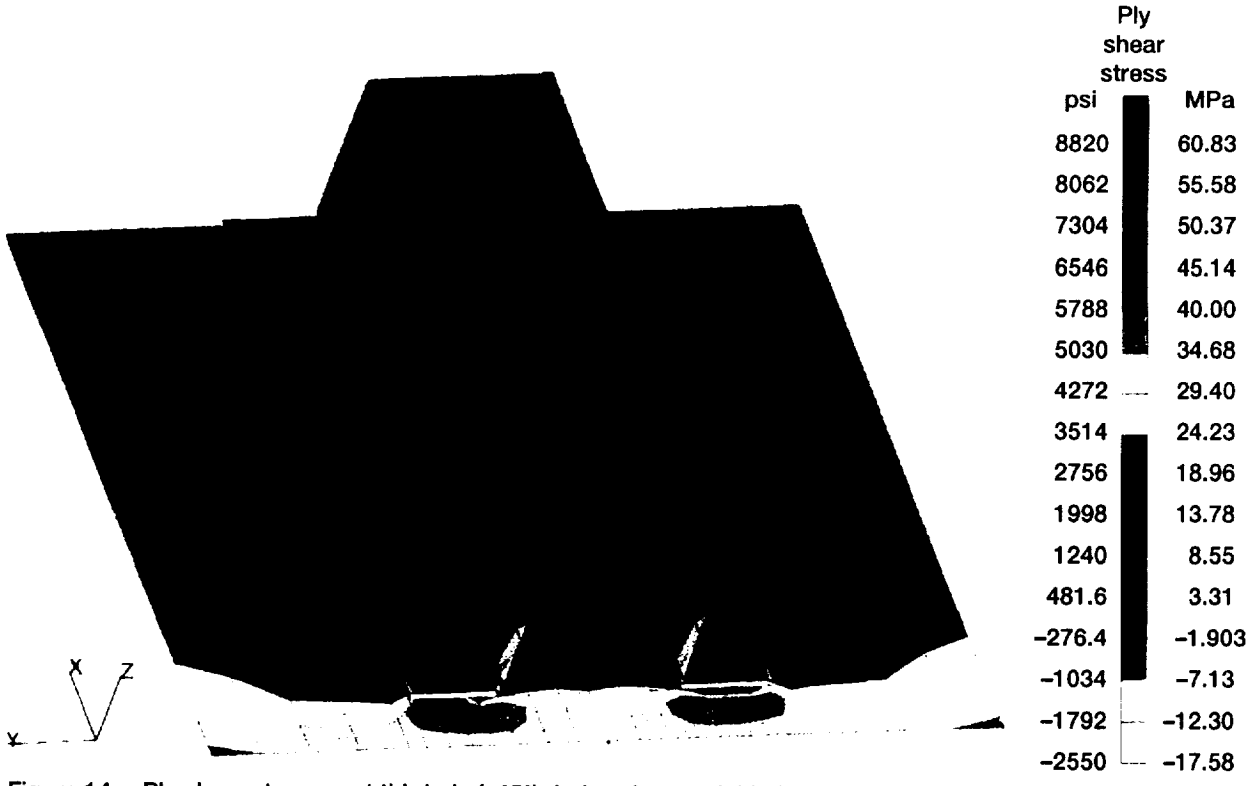

Figure 14.—Ply shear stresses at third ply (–45°) during damage initiation for graphite/epoxy panel $[0/\pm45/90]_{s6}$. Applied load, 974.5 N-m (8385 lb-in.).

REPORT DOCUMENTATION PAGE

Form Approved
OMB No. 0704-0188

1. AGENCY USE ONLY (*Leave blank*)	2. REPORT DATE	3. REPORT TYPE AND DATES COVERED
	September 1996	Technical Memorandum

4. TITLE AND SUBTITLE
Progressive Fracture of Fiber Composite Builtup Structures

5. FUNDING NUMBERS
WU-505-63-5B

6. AUTHOR(S)
Pascal K. Gotsis, C.C. Chamis, and Levon Minnetyan

7. PERFORMING ORGANIZATION NAME(S) AND ADDRESS(ES)
National Aeronautics and Space Administration
Lewis Research Center
Cleveland, Ohio 44135-3191

8. PERFORMING ORGANIZATION REPORT NUMBER
E-10269

9. SPONSORING/MONITORING AGENCY NAME(S) AND ADDRESS(ES)
National Aeronautics and Space Administration
Washington, DC 20546-0001

10. SPONSORING/MONITORING AGENCY REPORT NUMBER
NASA TM-107231

11. SUPPLEMENTARY NOTES
Prepared for the 32nd Annual Technical Meeting, sponsored by the Society of Engineering Science, New Orleans Louisiana, October 29–November 2, 1995. Pascal K. Gotsis and C.C. Chamis, NASA Lewis Research Center; Levon Minnetyan, Clarkson University, Potsdam, New York. Responsible person, Pascal K. Gotsis, organization code 5210, (216) 433–3331.

12a. DISTRIBUTION/AVAILABILITY STATEMENT
Unclassified - Unlimited
Subject Category 39

This publication is available from the NASA Center for AeroSpace Information, (301) 621–0390.

12b. DISTRIBUTION CODE

13. ABSTRACT ***(Maximum 200 words)***

The damage progression and fracture of builtup composite structures was evaluated by using computational simulation to examine the behavior and response of a stiffened composite $[0/\pm45/90]_{s6}$ laminate panel subjected to a bending load. The damage initiation, growth, accumulation, progression, and propagation to structural collapse were simulated. An integrated computer code (CODSTRAN) was augmented for the simulation of the progressive damage and fracture of builtup composite structures under mechanical loading. Results showed that damage initiation and progression have a significant effect on the structural response. Also investigated was the influence of different types of bending load on the damage initiation, propagation, and final fracture of the builtup composite panel.

14. SUBJECT TERMS
Laminated thin shells; Fiber composite structures; Computational simulation; Structural analysis; Finite element analysis; Damage; Degradation; Durability; Fracture; Stiffened panel; Structural degradation.

15. NUMBER OF PAGES
14

16. PRICE CODE
A03

17. SECURITY CLASSIFICATION OF REPORT	18. SECURITY CLASSIFICATION OF THIS PAGE	19. SECURITY CLASSIFICATION OF ABSTRACT	20. LIMITATION OF ABSTRACT
Unclassified	Unclassified	Unclassified	